PHYSICO-CHEMICAL BASICS OF METALLURGICAL PROCESSES / ФИЗИКО-ХИМИЧЕСКИЕ ОСНОВЫ МЕТАЛЛУРГИЧЕСКИХ ПРОЦЕССОВ

UDC 669.168
DOI 10.17073/0368-0797-2023-4-471-478

Original article
Оригинальная статья

PHYSICAL PROPERTIES AND STRUCTURE OF BORON-CONTAINING SLAGS DURING REDUCTION PERIOD OF AOD PROCESS

R. R. Shartdinov, A. A. Babenko, A. G. Upolovnikova, A. N. Smetannikov

Institute of Metallurgy, Ural Branch of the Russian Academy of Sciences (101 Amundsena Str., Yekaterinburg 620016, Russian Federation)

rr.shartdinov@gmail.com

Abstract. The effect of basicity and content of boron oxide on viscosity, crystallization temperature, phase composition, and structure of the $CaO–SiO_2–B_2O_3$ – 12 % Cr_2O_3 – 3 % Al_2O_3 – 8 % MgO fluorine-free slag system in the range of boron oxide content 3 – 6 % and basicity 1.0 – 2.5 is studied by vibrational viscometry, thermodynamic phase composition modeling (HSC Chemistry 6.12 (Outokumpu)), and Raman spectroscopy. It was found that physical properties of the studied slags mainly depend on the balance between the degree of structure polymerization, nature of the bond with it, and phase composition. With a low basicity of 1.0, slags are "long" and an increase in the content of boron oxide from 3 to 6 % makes them more fusible, reducing the crystallization temperature of the slag from 1340 to 1224 °C, and its viscosity from 1.0 – 0.8 to ~0.25 Pa·s at 1600 – 1660 °C, despite the significant complication of the structure, reflected in the growth of the bridging oxygen index BO from 1.10 to 1.49. With an increase in basicity, slags transfer from "long" to "short" and the content of calcium oxide increases, which, being a donor of free oxygen ions (O^{2-}), acts as a modifier of the slag structure. Thus, with a basicity of $B = (CaO/SiO_2) = 2.5$, slags have a simpler structure (BO = 0.50 – 0.53) relative to slags with a basicity of 1.0, while the addition of boron oxide complicates it only slightly (an increase in BO from 0.5 up to 0.53). Increasing the concentration of B_2O_3 lowers the crystallization temperature from 1674 to 1605 °C and the viscosity from 1.0 to 0.3 Pa·s at 1660 °C as a result of the formation of low-melting compounds (mostly $2CaO·B_2O_3$).

Keywords: AOD-slag, boron oxide, chromium oxide, structure, viscosity, phase composition, crystallization temperature

Acknowledgements: The work was performed as part of the state task of the Institute of Metallurgy of the Ural Branch of the Russian Academy of Sciences using the equipment of the CCP "Composition of Matter" of the Institute of High-Precision Electronics of the Ural Branch of the Russian Academy of Sciences.

For citation: Shartdinov R.R., Babenko A.A., Upolovnikova A.G., Smetannikov A.N. Physical properties and structure of boron-containing slags during reduction period of AOD process. *Izvestiya. Ferrous Metallurgy*. 2023;66(4):471–478.
https://doi.org/10.17073/0368-0797-2023-4-471-478

ФИЗИЧЕСКИЕ СВОЙСТВА И СТРУКТУРА БОРСОДЕРЖАЩИХ ШЛАКОВ ВОССТАНОВИТЕЛЬНОГО ПЕРИОДА АКР-ПРОЦЕССА

Р. Р. Шартдинов, А. А. Бабенко, А. Г. Уполовникова, А. Н. Сметанников

Институт металлургии Уральского отделения Российской академии наук (Россия, 620016, Свердловская обл., Екатеринбург, ул. Амудсена, 101)

rr.shartdinov@gmail.com

Аннотация. Влияние основности и содержания оксида бора на вязкость, температуру кристаллизации, фазовый состав и структуру безфтористых шлаков системы $CaO–SiO_2–B_2O_3$ – 12 % Cr_2O_3 – 3 % Al_2O_3 – 8 % MgO в диапазоне содержания оксида бора от 3 до 6 % и основности 1,0 – 2,5 были изучены посредством вибрационной вискозиметрии, термодинамического моделирования фазового состава (HSC Chemistry 6.12 (Outokumpu)) и рамановской спектроскопии. Было установлено, что физические свойства изучаемых шлаков главным образом зависят от баланса между степенью полимеризации структуры, природы связи в ней и фазового состава. При низкой основности (примерно 1,0) шлаки являются «длинными» и рост содержания оксида бора с 3 до 6 % делает их более легкоплавкими, снижая температуру кристаллизации шлака с 1340 до 1224 °C, а вязкость – с 1,0 – 0,8 примерно до 0,25 Па·с при температуре 1600 – 1660 °C, несмотря на значительное усложнение структуры, отражающееся в росте показателя мостикового кислорода BO с 1,10 до 1,49. С повышением основности шлаки из «длинных» переходят в «короткие». Растет содержание оксида кальция, который, являясь донором свободных ионов кислорода (O^{2-}), выступает в роли модификатора структуры шлака. При основности $B = (CaO/SiO_2) = 2,5$ шлаки обладают более

простой структурой (ВО = 0,50 – 0,53) относительно шлаков с основностью 1,0, при этом добавление оксида бора усложняет ее лишь незначительно (рост показателя ВО с 0,50 до 0,53). Увеличение концентрации B_2O_3 понижает температуру кристаллизации с 1674 до 1605 °С и вязкость – с 1,0 до 0,3 Па·с при температуре 1660 °С в результате образования легкоплавких соединений ($2CaO·B_2O_3$).

Ключевые слова: АКР-шлак, оксид бора, оксид хрома, структура, вязкость, фазовый состав, температура кристаллизации

Благодарности: Работа выполнена в рамках исполнения государственного задания Института металлургии Уральского отделения Российской академии наук с использованием оборудования ЦКП «Состав вещества» Института высокоточной электроники Уральского отделения Российской академии наук.

Для цитирования: Шартдинов Р.Р., Бабенко А.А., Уполовникова А.Г., Сметанников А.Н. Физические свойства и структура борсодержащих шлаков восстановительного периода АКР-процесса. *Известия вузов. Черная металлургия*. 2023;66(4):471–478.
https://doi.org/10.17073/0368-0797-2023-4-471-478

Introduction

Currently, the primary method employed for the smelting of low-carbon stainless steel is the argon oxygen decarburization (AOD). This technology, originated by Union Carbide Corp. in the USA in 1968, became widely adopted, and by the onset of the 21st century, approximately three-quarters of all stainless steel production used this technique [1].

The AOD process consists of two distinct phases: oxidation and reduction. The primary objective of the oxidation period is to decarbonize the metal by introducing a mixture of oxygen and inert gas, thereby attaining the required carbon concentrations while minimizing the oxidation of chromium. Subsequently, the reduction period ensues, during which the metal is purged solely with inert gas to enhance mixing and reintegrate oxidized chromium into the metal, accomplished through the addition of aluminum or silicon additives. Concluding the reduction phase, the metal undergoes desulfurization, resulting in the formation of slag characterized by low FeO oxide content and a basicity ranging from 2.0 to 2.5 [1]. Nevertheless, the effectiveness of achieving profound metal desulfurization and the efficient reduction of chromium is not solely dependent on the chemical activity of the oxide system components; it also relies on creating favorable kinetic conditions for the processes [1 – 3].

The kinetics of the processes involved in metal desulfurization and chromium reduction are predominantly influenced by the fluid mobility of the generated slags [1; 4]. The diffusion rates of sulfur and chromium oxide within the slag are inversely proportional to its viscosity [2]. To promote low viscosity in the resultant slag, fluorspar is frequently employed as a flux [1; 5; 6]. However, the utilization of the CaF_2 compound poses a significant drawback due to the generation of environmentally harmful volatile fluorides at elevated temperatures during the process [3; 7]. The advancement of this process is accompanied by a reduction in the refining properties of the resulting slags, an escalation in environmental impact, and a corrosive effect on equipment. Therefore, there is a need to develop refining slags with enhanced fluid mobility that do not incorporate fluorspar. A viable solution to this challenge is the incorporation of boron oxide, which, through interactions with the primary components of the generated slags, forms low melting eutectics ($CaO·B_2O_3$ and $2CaO·B_2O_3$ with melting points of 1130 and 1280 °C), ensuring heightened fluid mobility.

In this study, the viscosity (η), crystallization temperature (t_{cr}), phase composition, and structure of slags in the $CaO – SiO_2 – B_2O_3 – 12$ % $Cr_2O_3 – 3$ % $Al_2O_3 – 8$ % MgO system were investigated across a range of boron oxide content from 3 to 6 % and basicity levels of 1.0 – 2.5. This investigation employed vibration viscometry, thermodynamic simulation of phase composition (HSC Chemistry 6.12 (Outokumpu)), and Raman spectroscopy.

Materials and experimental methods

In order to investigate the properties of slags within the $CaO–SiO_2–B_2O_3–12$ % $Cr_2O_3–3$ % $Al_2O_3–8$ % MgO system, slags were prepared, and their composition outlined in Table 1.

Table 1

Composition of the experimental slags

Таблица 1. **Состав экспериментальных шлаков**

Slag sample	Content in slag, %						*B*	t_{cr}, °C
	CaO	SiO_2	B_2O_3	MgO	Al_2O_3	Cr_2O_3		
1	37.00	37.00	3	8	3	12	1.0	1340
2	52.86	21.14	3	8	3	12	2.5	1674
3	50.71	20.29	6	8	3	12	2.5	1605
4	35.50	35.50	6	8	3	12	1.0	1224

The slag was melted in a resistance furnace using molybdenum crucibles in an argon atmosphere, with oxides of analytical grade calcined for 2 – 3 h at a temperature of 800 °C (oxide B_2O_3 at 100 °C).

Viscosity measurements of the resulting slags were conducted employing a vibration viscometer [8] in molybdenum crucibles under an argon atmosphere. Temperature measurement was executed using a tungsten–rhenium thermocouple. The data obtained, characterizing slag viscosity as a function of temperature, were utilized to construct graphs in $\ln\eta - 1/T$ coordinates. The inflection point of the viscosity polytherms in these coordinates, following Frenkel's theory of viscous flow, indicates the temperature at which slag crystallization initiates [9].

Thermodynamic simulation of the phase composition of experimental slag samples was performed using the HSC Chemistry 6.12 software package (Outokumpu) [10].

The structure of experimental slag samples was examined using a U 1000 Raman microscope-spectrometer with a laser featuring an exciting wavelength of 532 nm. The resulting spectra are presented graphically within the wavenumber range of 400 – 1500 cm^{-1}.

Results and discussion

The measured viscosity of the slags within the oxide system under investigation is illustrated in Fig. 1, and in Fig. 2, they are depicted in $\ln\eta - 1/T$ coordinates; the onset temperature of crystallization was determined based on the inflection in the dependency (Table 1).

Throughout the study, Raman spectra of the examined slags *1* – *4* were acquired (Fig. 3).

It is postulated that the extent of slag polymerization is primarily influenced by the high-frequency silicate range of 800 – 1200 cm^{-1}, corresponding to $[SiO_4]$ tetrahedra. For a comprehensive understanding of the slag structure, deconvolution of the Raman spectra within this range was conducted using the Gaussian method [11]. The distinctive peaks of elements Q^n_{Si} ($[SiO_4]$ with the number of bridging oxygen n) and others are detailed in Table 2, with the results of the deconvolution presented in Fig. 4.

A plausible method for representing the degree of slag polymerization is through the average quantity of bridging oxygen (BO). This metric is articulated as the number of bridging oxygen atoms multiplied by the relative

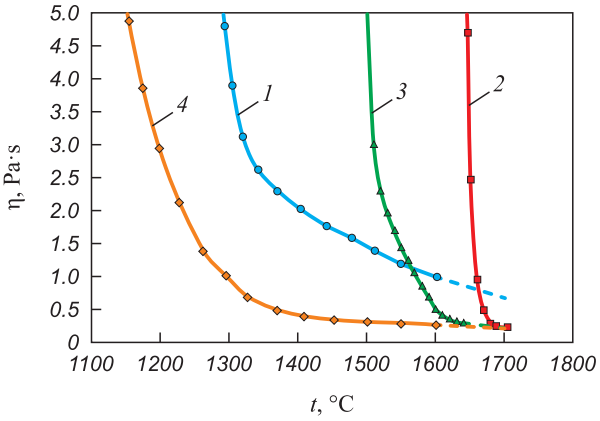

Fig. 1. Dependence of slag viscosity (*1* – *4*) on temperature

Рис. 1. Зависимость вязкости шлаков (*1* – *4*) от температуры

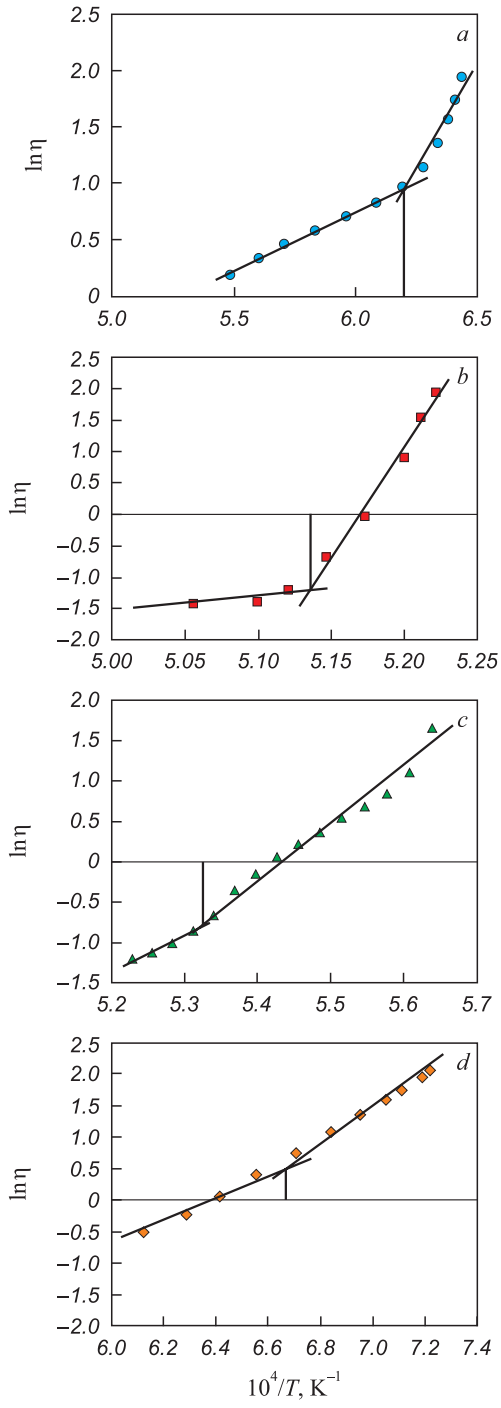

Fig. 2. Dependence of the logarithm of viscosity (lnη) on the inverse absolute temperature (1/*T*) for slags *1* – *4* (*a* – *d*)

Рис. 2. Зависимость логарифма вязкости (lnη) от обратной абсолютной температуры (1/*T*) для шлаков *1* – *4* (*a* – *d*)

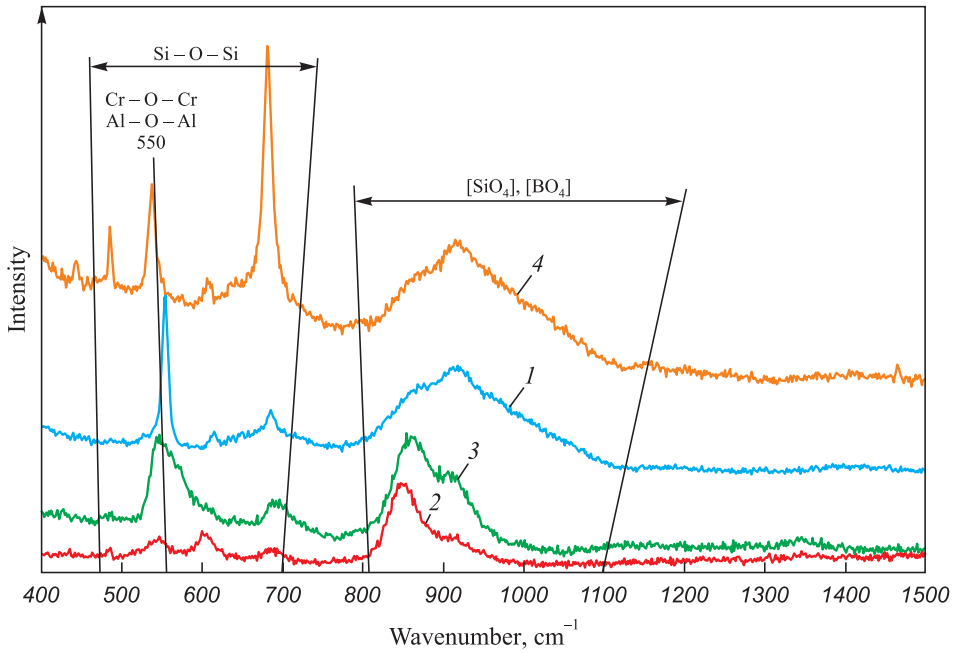

Fig. 3. Raman spectra of the slag samples *1* (B = 1.0; 3 % B_2O_3), *2* (B = 2.5; 3 % B_2O_3), *3* (B = 2.5; 6 % B_2O_3), *4* (B = 1.0; 6 % B_2O_3)

Рис. 3. Рамановские спектры образцов шлаков *1* (B = 1,0; 3 % B_2O_3), *2* (B = 2,5; 3 % B_2O_3), *3* (B = 2,5; 6 % B_2O_3), *4* (B = 1,0; 6 % B_2O_3)

fraction of each structural unit [SiO_4] and is calculated using the formula outlined in Table 3:

$$BO = 0 \cdot Q^0_{Si} + 1 \cdot Q^1_{Si} + 2 \cdot Q^2_{Si} + 3 \cdot Q^3_{Si} + 4 \cdot Q^4_{Si}.$$

Table 4 showcases the outcomes of the thermodynamic simulation of the phase composition of experimental slag samples. The results, determined by the melting temperatures of the formed phases, were categorically divided into three groups: low temperature (1130 – 1280 °C), medium temperature (1460 – 1600 °C), and high temperature (1710 – 2852 °C) phases.

Acidic slags with a basicity of 1.0 (samples *1* and *4*) fall into the category of "long" slags (Fig. 1), characterized by a high degree of polymerization (Table 3). Fig. 3 does not display peaks corresponding to the [BO_3] compound. It can be inferred that the B_2O_3 oxide is incorporated into the structure through 3D tetrahedra of the [BO_4] compound, aligning with wave numbers of 900 – 920 cm^{-1} (Table 2).

As per the deconvolution results, slag 1, with a basicity of 1.0 and 3 % B_2O_3, possesses a BO index value of 1.1. Its structure is predominantly represented by the [SiO_4] compound without bridging oxygen, along with 1

Table 2

Correspondence of wave numbers and structures

Таблица 2. **Соответствие волновых чисел и структур**

Element	Wavenumber, cm^{-1}	Structure	References
Q^0_{Si}	850 – 880	w/o bridging oxygen in [SiO_4]	[12; 13]
Q^1_{Si}	900 – 920	with one o bridging oxygen in [SiO_4]	
Q^2_{Si}	950 – 980	with two o bridging oxygens in [SiO_4]	
Q^3_{Si}	1040 – 1060	with three o bridging oxygens in [SiO_4]	
Q^4_{Si}	1060, 1190	with four o bridging oxygens in [SiO_4]	
Si – O – Si	500 – 650	Si – O^0 symmetric deformation vibrations	[14]
Al – O – Al	550	Al – O^0 vibrations	[15]
Cr – O – Cr	520 – 540	Cr – O^0 non-symmetric valence vibrations	[16]
[BO_3]	1350 – 1530	B – O^- valence vibrations in [BO_3]$^-$	[17; 18]
[BO_4]	900 – 920	B – O^0 symmetric valence vibrations in [BO_4]	[18]

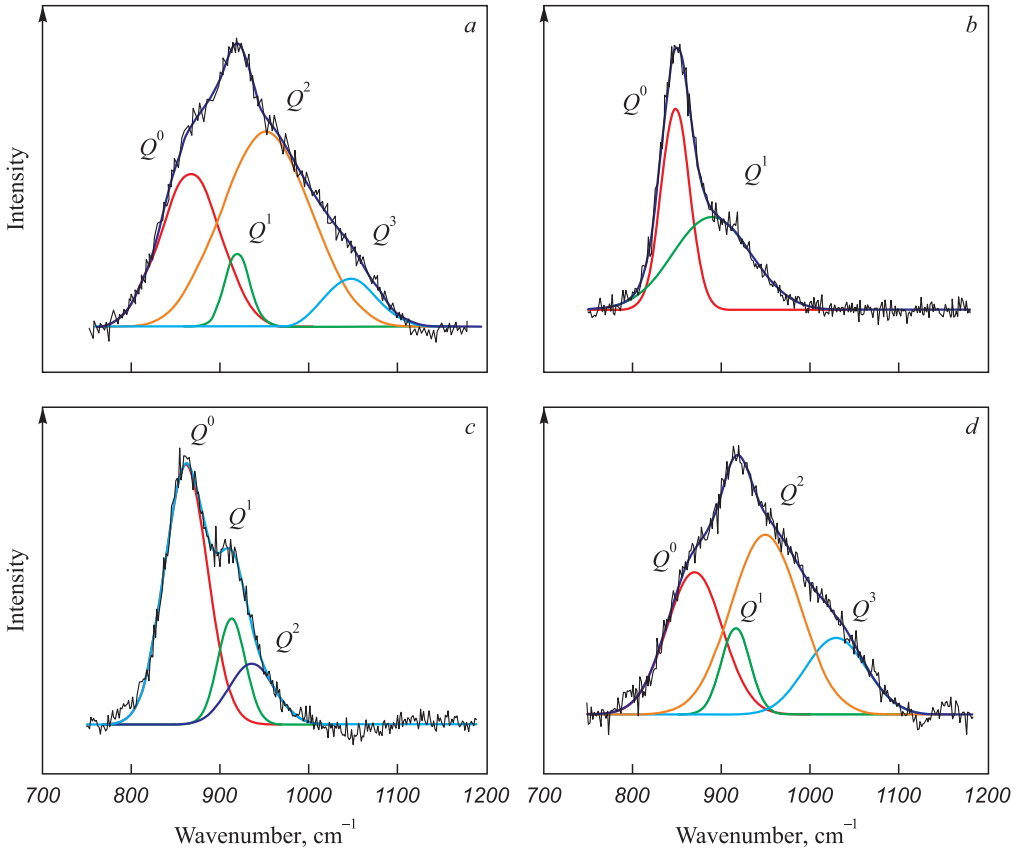

Fig. 4. Deconvolated spectra for the slags *1 – 4* (*a – d*)

Рис. 4. Деконволированные спектры для шлаков *1 – 4* (*a – d*)

and 2 bridging oxygen, with proportions of 0.39, 0.17 and 0.41, respectively. The combination of a relatively complex silicon–oxygen network structure (BO = 1.1) with a high concentration of high-temperature phases (32.23 %) leads to the formation of slag characterized by high viscosity of 1.0 – 0.8 Pa·s at 1600 – 1660 °C and a crystallization temperature of 1340 °C (Table 1).

Increasing the boron oxide content to 6 % induces even greater polymerization in slag *4* (BO = 1.49). This leads to an elevated proportion of Q^2 (0.45) and Q^3 (0.17), primarily due to changes in Q^0 and Q^1 values. At the same time, the proportion of low-melting compounds in the slag rises to 26.3 %, while the content of high-temperature phases decreases to 30.66 %. Despite the presence of a more intricate silicon-oxygen structure (BO = 1.49), in the form of [BO_4] tetrahedra, weakens the complex silicon-oxygen lattice. This weakening occurs as the resulting B – O^0 bonds are weaker than the Si – O^0 bonds. This "weakening" of the slag structure, combined with an increase in the proportion of low-melting compounds, results in a reduced viscosity of slag *4* to approximately 0.25 Pa·s at a temperature of 1600 – 1660 °C.

Table 3

Fractions of silicate structural elements

Таблица 3. **Доли силикатных структурных элементов**

Slag sample	Structural element				BO
	Q^0_{Si}	Q^1_{Si}	Q^2_{Si}	Q^3_{Si}	
1	0.39	0.17	0.41	0.03	1.10
2	0.50	0.50	0	0	0.50
3	0.63	0.21	0.16	0	0.53
4	0.29	0.09	0.45	0.17	1.49

Slags *2* and *3*, characterized by high basicity of 2.5, exhibit a "shorter" nature with a low degree of polymerization (refer to Fig. 1 and Table 3). As the basicity of these slags increases to 2.5, the peak in the silicate region of the spectrum (800 – 1200 cm^{-1}) shifts towards a decrease in wavenumber (Fig. 3). This shift is attributed to calcium oxide (CaO), acting as a slag structure modifier by providing free oxygen ions (O^{2-}). These free oxygen ions react with bridging oxygen (O^0) in silicates, resulting in a reduction in the complexity of Si–O bonds in the slag structure. Consequently, an increase in CaO content promotes the development of the depolymerization process [19 – 23]. Peaks in the wavenumber range of 500 – 650 cm^{-1} correspond to the Cr – O – Cr, Si – O – Si and Al – O – Al bonds. With an increase in

Table 4

Phase composition of the experimental slags at 1650 °C

Таблица 4. **Фазовый состав экспериментальных шлаков при температуре 1650 °C**

Phases	Fusing temperature, °C	Phase content in slag sample, %			
		1	*2*	*3*	*4*
Low temperature phases					
$CaO·B_2O_3$	1130	1.88	0.06	0.28	4.10
$2CaO·B_2O_3$	1280	4.47	2.81	7.55	8.22
$CaO·MgO·2SiO_2$	1391	13.49	0.07	0.22	13.95
Total		19.84	2.94	8.05	26.27
Medium temperature phases					
$2CaO·MgO·2SiO_2$	1454	4.35	0.43	0.83	3.77
$3CaO·B_2O_3$	1460	0.52	6.46	10.09	0.80
$3CaO·2SiO_2$	1460	9.76	5.89	6.69	7.18
$CaO·MgO·SiO_2$	1503	8.93	5.17	6.98	8.39
$3CaO·Al_2O_3$	1539	0	0.44	0.12	0
$CaO·SiO_2$	1540	17.99	3.22	4.37	17.06
$CaO·Al_2O_3·SiO_2$	1550	0.45	0.03	0.06	0.42
$CaO·Al_2O_3·2SiO_2$	1550	2.71	0	0.01	2.80
$3CaO·MgO·2SiO_2$	1575	2.14	4.18	4.72	1.56
$2CaO·Al2O_3·SiO_2$	1590	0.67	0.89	1.00	0.53
$CaO·Al_2O_3$	1600	0.27	2.10	1.64	0.23
Total		47.77	28.81	36.52	42.75
High temperature phases					
SiO_2	1710	4.70	0.04	0.10	5.31
$2MgO·SiO_2$	1890	1.19	0.11	0.26	1.32
Al_2O_3	2040	0.74	0.29	0.39	0.76
$3CaO·SiO_2$	2070	0.06	4.22	1.94	0.04
$CaO·Cr_2O_3$	2100	5.49	14.92	14.00	4.80
$2CaO·SiO_2$	2130	9.61	34.04	26.89	7.66
$MgO·Al_2O_3$	2135	0.86	1.10	1.47	0.87
Cr_2O_3	2435	7.99	1.10	1.77	8.33
CaO	2570	0.24	5.04	2.77	0.21
MgO	2852	1.34	4.56	4.27	1.36
Total		32.23	65.43	53.86	30.66

basicity, these peaks smooth out, indicating a weakening of the bonds.

Slag *2*, containing 3 % boron oxide, possesses the least complex structure (BO = 0.5). It is characterized by an equal number of Q^0 and Q^1 values featuring a simple silicon-oxygen structure with a small amount of bridging oxygen. The slag is distinguished by a high proportion of refractory phases (more than 65 %) and a small proportion of low-melting phases (2.94 %). Consequently, its crystallization temperature is 1676 °C, and viscosity is 1.0 Pa·s at a temperature of 1660 °C.

Increasing the boron oxide content to 6 % in slag *3* has virtually no effect on its polymerization compared to slag *2* (the amount of bridging oxygen does not exceed 0.53). The structure contains Q^0, Q^1 and Q^2, with proportion of 0.63, 0.21 and 0.16, respectively. However, an increase in the content of low-melting phases to 8.05 % and a decrease in the proportion of refractory phases to 53.86 % positively influence the crystallization temperature (1605 °C) and slag viscosity, which decreased to 0.5 – 0.3 Pa·s in the range of 1600 – 1660 °C.

The obtained data on the influence of slag basicity and boron oxide content on phase composition, structure, viscosity, and crystallization temperature highlight that slag viscosity depends on the balance between the degree of polymerization of the structure, the nature of the bonds within it, and the phase composition.

Conclusions

The study has yielded new data on the impact of basicity and boron oxide content on the viscosity, crystallization temperature, phase composition, and structure of slags within the $CaO–SiO_2–B_2O_3$ – 12 % Cr_2O_3 – 3 % Al_2O_3 – 8 % MgO system, spanning a range of boron oxide content from 3 to 6 % and basicity from 1.0 to 2.5.

The findings reveal that the physical properties of the investigated slags predominantly hinge on the delicate equilibrium between the degree of polymerization of the structure, the nature of the bonds within it, and the phase composition. At a low basicity of 1.0, augmenting the boron oxide content from 3 to 6 % renders the slag more fusible, leading to a reduction in the crystallization temperature from 1340 to 1224 °C and a decrease in viscosity from 1.0 – 0.8 to approximately 0.25 Pa·s at a temperature of 1600 – 1660 °C. This occurs despite a notable increase in structural complexity, as reflected in the rise of the BO index from 1.10 to 1.49.

In the case of high basicity (B = 2.5), the slags exhibit a simpler structure (BO = 0.50 – 0.53), and the addition of boron oxide only marginally complicates it (from 0.50 to 0.53). An increase in B_2O_3 content results in a reduction of the crystallization temperature from 1674 to 1605 °C and a decrease in viscosity from 1.0 to 0.3 Pa·s at a temperature of 1660 °C, attributed to the formation of low-melting compounds.

References / Список литературы

1. Tokovoi O.K. *Argon Oxygen Refining of Stainless Steel*. Chelyabinsk: ITs YuUrGU; 2015:250. (In Russ.).

Токовой О.К. *Аргонокислородное рафинирование нержавеющей стали*. Челябинск: ИЦ ЮУрГУ; 2015:250.

2. Popel' S.I., Sotnikov A.I., Boronenkov V.N. *Theory of Metallurgical Processes*. Moscow: Metallurgiya; 1986:463. (In Russ.).

   Попель С.И., Сотников А.И., Бороненков В.Н. *Теория металлургических процессов*. Москва: Металлургия; 1986:463.
3. Dyudkin D.A., Kisilenko V.V. *Production of Steel. In 3 vols. Vol. 3. Out-of-Furnace Steel Metallurgy*. Moscow: Teplotekhnik; 2010:544. (In Russ.).

   Дюдкин Д.А., Кисиленко В.В. *Производство стали. В 3-х томах. Т. 3. Внепечная металлургия стали*. Москва: Теплотехник; 2010:544.
4. Yavoiskii V.I., Yavoiskii A.V. *Scientific Foundations of Modern Production Processes of Steel*. Moscow: Metallurgiya; 1987:184. (In Russ.).

   Явойский В.И., Явойский А.В. *Научные основы современных процессов производства стали*. Москва: Металлургия; 1987:184.
5. Magidson I.A., Morozov A.S., Sidorenko M.F., etc. Viscosity of chromium slags. *Izvestiya. Ferrous Metallurgy*.1973;16(11):61–64. (In Russ.).

   Магидсон И.А., Морозов А.С., Сидоренко М.Ф. и др. Вязкость хромистых шлаков. *Известия вузов. Черная металлургия*. 1973;16(11):61–64.
6. Kalicka Z., Kawecka-Cebula E., Pytel K. Application of the Iida model for estimation of slag viscosity for Al_2O_3–Cr_2O_3–CaO–CaF_2 systems. *Archives of Metallurgy and Materials*. 2009;54(1):179–187.
7. Povolotskii D.Ya., Roshchin V.E., Gribanov V.P., etc. Influence of SiO_2 on the volatility of slags of Al_2O_3–Al_2O_3–CaF_2 system. *Izvestiya. Ferrous metallurgy*. 1982;25(8):39–42. (In Russ.).

   Поволоцкий Д.Я., Рощин В.Е., Грибанов В.П. и др. Влияние SiO_2 на летучесть шлаков системы Al_2O_3–Al_2O_3–CaF_2. *Известия вузов. Черная металлургия*. 1982;25(8):39–42.
8. Shtengel'meier S.V., Prusov V.A., Bogechov V.A. Improving viscosity measuring with a vibration viscometer. *Zavodskaya laboratoriya*. 1985;(9):56–57. (In Russ.).

   Штенгельмейер С.В., Прусов В.А., Богечов В.А. Усовершенствование методики измерения вязкости вибрационным вискозиметром. *Заводская лаборатория*. 1985;9:56–57.
9. Voskoboinikov V.G., etc. *Properties of Blast Furnace Slags*. Moscow: Metallurgiya; 1975:180. (In Russ.).

   Воскобойников В.Г. и др. *Свойства доменных шлаков*. Москва: Металлургия; 1975:180.
10. Roine A. *HSC 6.0 Chemistry Reactions and Equilibrium Software with Extensive Thermochemical Database and Flowshut*. Pori.: Outokumpu research Oy; 2006:448.
11. Mysen B.O., Virgo D., Scarfe C.M. Relations between the anionic structure and viscosity of silicate melts-a Raman spectroscopic study. *American Mineralogist*. 1980;65(7): 690–710.
12. McMillan P. Structural studies of silicate glasses and melts-applications and limitations of Raman spectroscopy. *American Mineralogist*. 1984;69(6):622–644.
13. Matson D.W., Sharma S.K., Philpotts J.A. The structure of high-silica alkali-silicate glasses. A Raman spectroscopic investigation. *Journal of Non-Crystalline Solids*. 1983;58(2-3): 323–352. https://doi.org/10.1016/0022-3093(83)90032-7
14. McMillan P.F., Poe B.T., Gillet P.H., Reynard B. A study of SiO_2 glass and supercooled liquid to 1950 K via high-temperature Raman spectroscopy. *Geochimica et Cosmochimica Acta*. 2001;58(17):3653–3662. https://doi.org/10.1016/0016-7037(94)90156-2
15. Kim T.S., Park J.H. Structure-viscosity relationship of low-silica calcium aluminosilicate melts. *ISIJ International*. 2014;54(9):2031–2038. https://doi.org/10.2355/isijinternational.54.2031
16. Dines T.J., Inglis S. Raman spectroscopic study of supported chromium (VI) oxide catalysts. *Physical Chemistry Chemical Physics*. 2003;5(6):1320–1328. https://doi.org/10.1039/b211857b
17. Kim Y., Morita K. Relationship between molten oxide structure and thermal conductivity in the CaO–SiO_2–B_2O_3 system. *ISIJ International*. 2014;54(9):2077–2083. https://doi.org/10.2355/isijinternational.54.2077
18. Cochain B., Neuville D.R., Henderson G.S., McCammon C.A., Pinet O., Richet P. Effects of the iron content and redox state on the structure of sodium borosilicate glasses: A Raman, Mössbauer and boron K-Edge XANES spectroscopy study. *Journal of the American Ceramic Society*. 2012;95(3):962–971. https://doi.org/10.1111/j.1551-2916.2011.05020.x
19. Mysen B.O., Virgo D., Seifert F.A. The structure of silicate melts: Implications for chemical and physical properties of natural magma. *Reviews of Geophysics*. 1982;20(3): 353–382. https://doi.org/10.1029/RG020i003p00353
20. Mysen B.O. Relationships between silicate melt structure and petrologic processes. *Earth-Science Reviews*. 1990;27(4): 281–365. https://doi.org/10.1016/0012-8252(90)90055-Z
21. Mills K.C. The influence of structure on the physico-chemical properties of slags. *ISIJ International*. 1993;33(1): 148–155. https://doi.org/10.2355/isijinternational.33.148
22. Park J.H. Structure–property correlations of CaO–SiO_2–MnO slag derived from Raman spectroscopy. *ISIJ International*. 2012;52(9):1627–1636. https://doi.org/10.2355/isijinternational.52.1627
23. Park J.H. Composition-structure-property relationships of CaO–*M*O–SiO_2 (*M* = Mg^{2+}, Mn^{2+}) systems derived from micro-Raman spectroscopy. *Journal of Non-Crystalline Solids*. 2012;358(23):3096–3012. https://doi.org/10.1016/j.jnoncrysol.2012.08.014

Information about the Authors

Ruslan R. Shartdinov, *Junior Researcher of the Laboratory of Steel and Ferroalloys,* Institute of Metallurgy, Ural Branch of the Russian Academy of Sciences
ORCID: 0000-0003-0852-1161
E-mail: rr.shartdinov@gmail.com

Anatolii A. Babenko, *Dr. Sci. (Eng.), Prof., Chief Researcher of the Laboratory of Steel and Ferroalloys,* Institute of Metallurgy, Ural Branch of the Russian Academy of Sciences
ORCID: 0000-0003-0734-6162
E-mail: babenko251@gmail.com

Alena G. Upolovnikova, *Cand. Sci. (Eng.), Senior Researcher of the Laboratory of Steel and Ferroalloys,* Institute of Metallurgy, Ural Branch of the Russian Academy of Sciences
ORCID: 0000-0002-6698-5565
E-mail: upol.ru@mail.ru

Artem N. Smetannikov, *Junior Researcher of the Laboratory of Steel and Ferroalloys,* Institute of Metallurgy, Ural Branch of the Russian Academy of Sciences
ORCID: 0000-0001-9206-0905
E-mail: artem.smetannikov.89@mail.ru

Сведения об авторах

Руслан Рафикович Шартдинов, *младший научный сотрудник лаборатории стали и ферросплавов,* Институт Уральского отделения РАН
ORCID: 0000-0003-0852-1161
E-mail: rr.shartdinov@gmail.com

Анатолий Алексеевич Бабенко, *д.т.н., профессор, ведущий научный сотрудник,* Институт металлургии Уральского отделения РАН
ORCID: 0000-0003-0734-6162
E-mail: babenko251@gmail.com

Алена Геннадьевна Уполовникова, *к.т.н., старший научный сотрудник лаборатории стали и ферросплавов,* Институт Уральского отделения РАН
ORCID: 0000-0002-6698-5565
E-mail: upol.ru@mail.ru

Артем Николаевич Сметанников, *младший научный сотрудник лаборатории стали и ферросплавов,* Институт Уральского отделения РАН
ORCID: 0000-0001-9206-0905
E-mail: artem.smetannikov.89@mail.ru

Contribution of the Authors

R. R. Shartdinov – conducting the experiment, processing and analysis of the research results, writing and editing the text.
A. A. Babenko – scientific guidance, analysis of the research results, writing and editing the text.
A. G. Upolovnikova – modeling, analysis of the research results, editing the text.
A. N. Smetannikov – conducting the experiment, analysis of the research results.

Вклад авторов

Р. Р. Шартдинов – проведение эксперимента, обработка, анализ, написание статьи, редактирование статьи.
А. А. Бабенко – научное руководство, анализ результатов, написание статьи, редактирование статьи.
А. Г. Уполовникова – моделирование, анализ, редактирование статьи
А. Н. Сметанников – проведение эксперимента, анализ.

Received 18.04.2023
Revised 12.05.2023
Accepted 22.05.2023

Поступила в редакцию 18.04.2023
После доработки 12.05.2023
Принята к публикации 22.05.2023